NEW VIEWS OF PLANUM BOREUM INTERIOR IN A MIGRATED 3-D VOLUME OF SHARAD DATA.

N. E. Putzig[1], F. J. Foss II[2], B. A. Campbell[3], and R. J. Phillips[1]. [1]Southwest Research Institute, Boulder, CO; [2]Freestyle Analytical & Quantitive Services, LLC, Longmont, CO; [3]Smithsonian Institution, Washington, DC. Contact: nathaniel@putzig.com.

Introduction: We present a new three-dimensional (3-D) volume of radar data from observations taken by the Shallow Radar (SHARAD) instrument on 1579 orbits of the Mars Reconnaissance Orbiter (MRO). This volume encompasses the entirety of Planum Boreum, the dome of ice-rich deposits that forms the north polar cap of Mars, and it provides a greatly improved view of the internal structure from the surface to the base of the deposits at depths of ~2–3 km.

Previous 2-D work. Collective analysis of SHARAD radargrams (2-D images of power along track vs. delay time) in Planum Boreum has revealed a repeated sequence of broadly continuous layers, likely linked to ~1-Ma obliquity cycles [1, 2]. Spiral troughs have been shown to be giant aeolian bedforms that have been translating poleward since the layered deposits were about half their present thickness [3]. Unconformities and deep structure define a buried chasma to the east of the topographic saddle that separates Gemina Lingula from the main lobe of layered deposits [4]. Deeper still, diffuse returns extend down to the level where the Mars Advanced Radar for Subsurface and Ionospheric Sounding (MARSIS) obtains strong returns from a basal unit [5, 6].

Preliminary 3-D work. A geographically limited 3-D data volume constructed from 540 observations of eastern Planum Boreum with no geometric corrections [7] readily shows features such as the trough-translation paths, buried chasma, and basal-unit boundary that previously required painstaking effort to map with 2-D radargrams. The preliminary 3-D work facilitated the development of a means to mitigate ionospheric time delays (see next section) and other pre-processing concerns. With these improvements and full geographic coverage of Planum Boreum, we have now obtained the first 3-D volume results using an seismic imaging process known as *migration*. This technique properly positions reflectors in 3-D space, correcting the confusing projection of off-nadir returns into the planes of the 2-D radargrams. 3-D migration is revealing major structural features that were largely hidden in 2-D radargrams (Fig. 1).

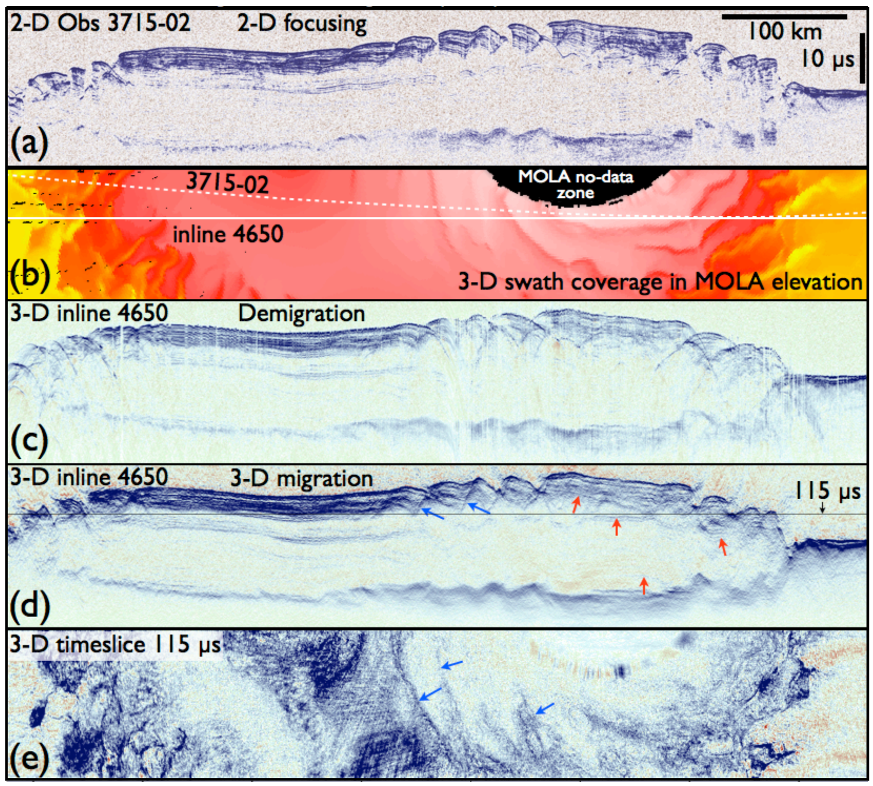

Figure 1. 3-D migration reveals new features within Planum Boreum. (a) 2-D radargram for SHARAD observation 3715-02 shows radar return power (blue high, red low), extending left to right across eastern Gemina Lingula, the main lobe, and into Olympia Planum. Subsurface reflectors are often obfuscated by interfering returns from off-nadir features and scattering losses, especially below trough-cut areas. (b) Map of SHARAD coverage at 3-km per pixel over a 3-D swath (yellow-red-white colors are low-to-high MOLA elevations), showing ground track for the single SHARAD observation in (a) and the 3-D inline in (c) and (d). (c) Radargram for 3-D inline 4650 after demigration to recover hyperbolic move-out of off-nadir returns. Residual timing differences discussed in text are discernible. (d) Radargram for 3-D inline 4650 after 3-D migration. Surface and subsurface geometry, including that of trough-translation paths (blue arrows), is corrected, and formerly hidden reflectors (red arrows) are revealed in areas most affected by off-nadir returns. (e) Timeslice at 115 μs from migrated 3-D radar swath. Trough-translation paths (blue arrows), structural boundaries, and other features are sharpened by the migration process.

SHARAD Observations: With a 10-MHz bandwidth centered at 20 MHz, SHARAD provides a range resolution of 15 m in free space, ~8 m in nearly pure water ice (expected for the Planum Boreum layered deposits [1, 8]), and still finer in ice with more lithic inclusions (expected in the basal deposits [9]). Lateral resolution at the surface is ~3–6 km, reducible along track to 0.3–1.0 km in processing [10]. High-power returns indicate a strong contrast in the dielectric properties of materials. In the polar terrains, the reflections likely arise from different degrees of dust or lithic loading between adjacent ice layers [1, 2, 11].

Off-nadir returns. Surface features such as crater walls and polar troughs located beyond the spacecraft's nadir point yield reflections, termed *clutter*, that can be difficult to distinguish from nadir returns. Internal structure (e.g., dipping layers) may result in the mislocation of features when using 2-D methods. While 2-D synthetic-aperture processing correctly positions reflectors in time delay, the relationship of delay to 3-D physical location differs among nadir and off-nadir surface and subsurface interfaces. In addition, the signal-to-noise ratio (SNR) can be low when material properties lead to substantial scattering or absorption.

SHARAD studies often use elevation data to simulate surface clutter for comparison to 2-D radargrams [e.g., 2, 12], but this technique does not mitigate clutter obfuscation of nadir subsurface returns, mispositioning of internal structures, and signal losses. However, with sufficient density of coverage, each of these issues can be alleviated with 3-D migration processing.

Time delays. Prior to applying migration, the along-track data must be corrected for any relative time delay introduced by the variable orbit altitude and the Martian ionosphere. While accurate ephemeris data enables a straightforward altitude correction, we found that the ionospheric delay varies significantly along track and from one orbit to another. A substantial effort produced an accurate method for estimating those delays [13], but residual delays up to ~0.2 μs remain (see Fig. 1). Investigation of a means to further reduce the timing delays is ongoing.

Migration Processing: The occurrence in seismic data of the geometric and loss concerns discussed above led to the development of migration, a mathematical inversion process that converts the recorded seismic image to one in which subsurface features appear in their proper position both laterally and vertically [14, 15]. Migration also improves resolution by collapsing backscattered wave-field energy to the scattering point. Many migration algorithms have been developed to account for various degrees of subsurface complexity [16-19]. As applied here, 3-D migration addresses many limitations of 2-D radargrams. For example, clutter returns are useful signals in 3-D space, enhancing the resulting image when repositioned to their source locations. Interfering returns are unraveled and internal structures are properly positioned. In addition, SNR improves by a combination of band-limited, spatial-domain processing and incoherent summation of reflectors seen in adjacent and crossing orbit tracks.

First Results: We applied an 2-D inverse-focusing process (demigration) to 1579 SHARAD tracks over Planum Boreum, collected these data into a volume, and applied 3-D Stolt migration [16]. Coverage in the 500×500-m designated bins ranges from 0 to ~40 tracks per bin, highest at the orbital tangent latitudes near 87°N. To reduce migration artifacts, we interpolated the data to fill empty bins. In Fig. 1, we present a vertical cut through the volume before (1c) and after (1d) migration, and a horizontal (constant delay-time) cut after migration (1e). The views of gross internal features such as the trough-translation paths, the buried chasma, the basal-unit boundary, and the diffuse basal unit itself are significantly sharpened by the migration processing. In addition, previously hidden features are revealed, such as the shallow sloping reflector in Fig. 1d that may be a major unconformity. This clearer view of the Planum Boreum interior provided by 3-D migration will advance understanding of the geologic history of the polar layered deposits and promises new insights into the development of Martian climate processes throughout the late Amazonian period.

References: [1] Phillips R. J. et al. (2008), *Science*, *320*, 1182–1185. [2] Putzig N. E. et al. (2009), *Icarus*, *204*, 443–457. [3] Smith I. B. et al. (2013), *J. Geophys. Res.*, *118*, doi:10.1002/jgre.20142, 1835–doi:10.1002/jgre.20142, 1857. [4] Holt J. W. et al. (2010), *Nature*, *465*, 446–449. [5] Selvans M. M. et al. (2009), *IEEE Radar Conf.* [6] Tanaka K. L. et al. (2008), *Icarus*, *196*, 318–358. [7] Putzig N. E. et al. (2012), *AGU Fall Meeting*. [8] Picardi G. et al. (2005), *Science*, *310*, 1925–1928. [9] Plaut J. J. et al. (2012), *Lunar Planet. Sci., XLIV*. [10] Seu R. et al. (2007), *J. Geophys. Res.*, *112*, E05S05. [11] Nunes D. C. and R. J. Phillips (2006), *J. Geophys. Res.*, *111*, E06S21. [12] Holt J. W. et al. (2008), *Science*, *322*, 1235–1238. [13] Campbell B. A. et al. (2014), *IEEE Geosci. Remote Sens. Lett.*, *11*, 632–635. [14] Claerbout J. F. (1985), *Imaging the Earth's Interior*, Blackwell Scientific Publications, Oxford, UK, 398 p. [15] Yilmaz O. (1987), *Seismic Data Processing*, Society of Exploration Geophysics, Tulsa, OK, 526 p. [16] Stolt R. H. (1978), *Geophysics*, *43*, 23. [17] Gazdag J. (1978), *Geophysics*, *43*, 1342–1351. [18] Gray S. H. et al. (2001), *Geophysics*, *66*, 1622–1640. [19] Bednar J. B. (2005), *Geophysics*, *70*, 3MJ–20MJ.